Ionization of medium-sized silicon clusters and the geometries of the cations

Bei Liu, Zhong-Yi Lu, Bicai Pan, Cai-Zhuang Wang, and Kai-Ming Ho
Ames Laboratory and Department of Physics and Astronomy, Iowa State University, Ames, Iowa 50011

Alexandre A. Shvartsburg and Martin F. Jarrold
Department of Chemistry, Northwestern University, 2145 Sheridan Road, Evanston, Illinois 60208

(Received 21 July 1998; accepted 28 August 1998)

We have performed a systematic ground state geometry search for the singly charged Si_n cations in the medium-size range ($n \leqslant 20$) using density functional theory in the local density approximation (LDA) and generalized gradient approximation (GGA). The structures resulting for $n \leqslant 18$ generally follow the prolate ''stacked Si_9 tricapped trigonal prism'' pattern recently established for the lowest energy geometries of neutral silicon clusters in this size range. However, the global minima of Si_n and Si_n^+ for $n=6$, 8, 11, 12, and 13 differ significantly in their details. For Si_{19} and Si_{20} neutrals and cations, GGA renders the prolate stacks practically isoenergetic with the near-spherical structures that are global minima in LDA. The mobilities in He gas evaluated for all lowest energy Si_n^+ geometries using the trajectory method agree with the experiment, except for $n=18$ where the second lowest isomer fits the measurements. The effect of gradient corrections for either the neutral or cationic clusters is subtle, but their inclusion proves to be critical for obtaining agreement with the mobility measurements in the $n=15-20$ range. We have also determined ionization potentials for our Si_n neutral geometries and found that all experimental size-dependent trends are reproduced for $n \leqslant 19$. This particularly supports our structural assignments for Si_9, Si_{11}, Si_{12}, and Si_{17} neutrals. The good overall agreement between the measured and calculated properties supports the elucidation of the ''prolate'' family of silicon clusters as stacks of trigonal prisms. © *1998 American Institute of Physics.* [S0021-9606(98)02445-3]

I. INTRODUCTION

An enormous theoretical effort has been invested over the last decade into the structural characterization of silicon clusters.[1–46] The geometries for small ($n \leqslant 7$) Si_n are now firmly established at both *ab initio*[1–8] and density functional[10–17] (DFT) levels and confirmed by Raman[47] and infrared (IR)[48] spectroscopy of matrix-isolated species, and vibrationally resolved photoelectron spectroscopy of gas-phase anions.[49a,b] They are a C_{2v} triangle for Si_3, a D_{2h} rhombus for Si_4, and D_{3h} trigonal, D_{4h} tetragonal, and D_{5h} pentagonal bipyramids for Si_5, Si_6, and Si_7, respectively (see Fig. 1). These compact, multiply coordinated structures are not fragments of the bulk silicon diamond lattice. Their reconstruction is driven by the energy gained by tying up the dangling bonds.

Calculations for slightly larger ($n=8-11$) clusters by Raghavachari and Rohlfing[3–7] (*ab initio*) and other researchers[11–14,18] using DFT revealed a close competition between growth patterns based on capping the octahedron and trigonal prism isomers of Si_6. For some time, the consensus has been that Si_8 is a C_{2h} distorted bicapped octahedron,[3–5,7,11,12,13a] Si_9 is either a C_s distorted tricapped octahedron[3–5,7] or a C_{2v} (II) distorted tricapped trigonal prism (TTP),[18,43] and Si_{10} is either a T_d tetracapped octahedron[3,4,6,7] or a C_{3v} tetracapped trigonal prism.[3,5–7,12,13a] However, the C_{2v} (I) capped Bernal's geometry[12] (a distorted capped cube) is now accepted[20,21] as the ground state of Si_9 neutral (see Fig. 1). Two isomers, both produced by capping a trigonal prism, have been proposed for Si_{11}: C_{2v}^5 and C_s (II).[19,20] Structural optimizations for $n=12$ and 13 found them to be a C_{2v} hexacapped trigonal prism[14,20] and a C_{3v} capped trigonal antiprism,[13,16,17,20,43] respectively. No *a priori* searches for $n>13$ have been reported, but several geometric families have been described that follow assumed bonding patterns. None of the structures for $n>7$ has been verified experimentally.

A number of properties for size-selected clusters larger than Si_7 have been measured in the gas phase, including photoelectron spectra of anions,[49,50] fragmentation pathways and dissociation energies of cations,[51–53] and ionization potentials of the neutrals.[54–57] However, the most information about the structure of the larger Si_n has been obtained by measuring the ionic mobilities for their cations.[58,59] These measurements have revealed that the clusters become prolate between $n=10$ and $n=23$, then a structural transition to a more spherical geometry occurs over the $n=24-34$ size range. Several different families of prolate clusters based on arbitrarily stacking hexagonal rings[41,42,45] or triangles[43] have been proposed, but none of them has the correct mobility.[60] We have recently performed an unbiased global optimization of Si_n neutrals with $n \leqslant 20$ employing the simulated annealing and genetic algorithm,[60] with the energies evaluated using DFT in the local density approximation (LDA). The geometries resulting for $n \leqslant 18$ were prolate, resembling stacks of Si_9 TTP.[61] The mobilities calculated for these structures were in a good agreement with the measurements.[60] The glo-

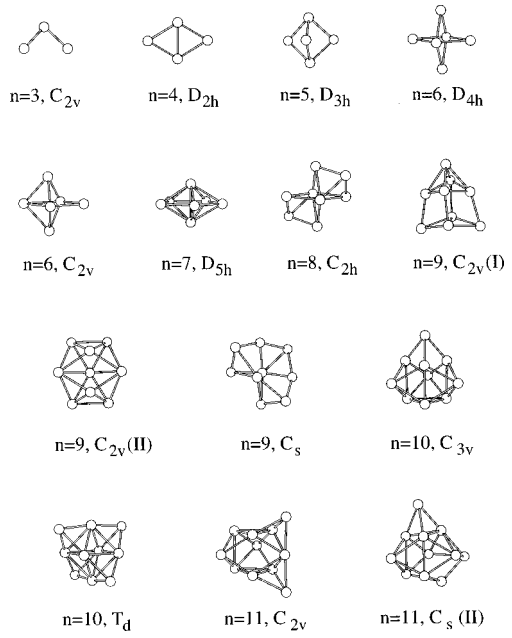

FIG. 1. Lowest energy geometries proposed for the Si_n ($n \leqslant 11$) neutrals in the literature.

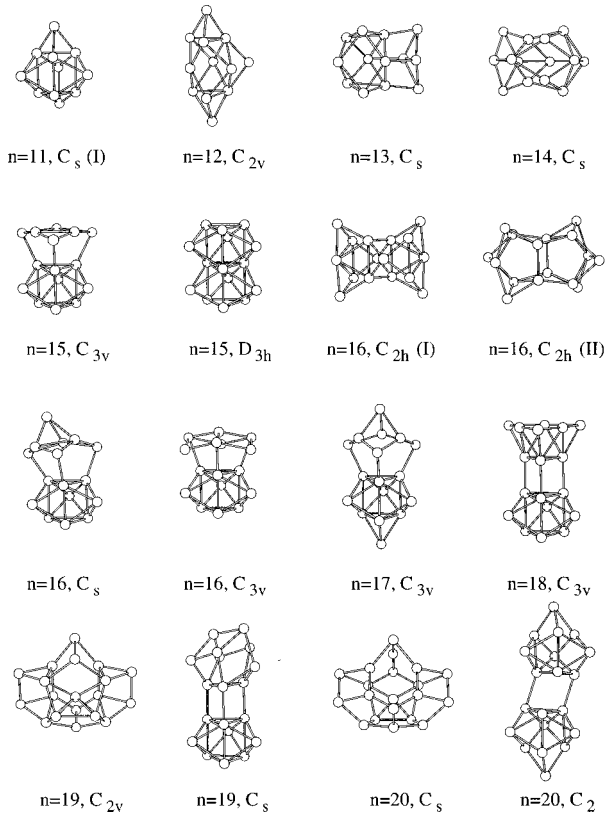

FIG. 2. Global minima for Si_n ($n=11-20$) neutrals and geometries lying within 5 meV/atom found in our LDA calculations. The lowest energy ''prolate'' structures for $n=19$ and 20 are also shown. The C_{2v} geometry for Si_{19} is identical to that labeled in Ref. 60 as C_s.

bal minima we found for $n=19$ and 20 were very different—they had near-spherical geometries. The mobilities calculated for these structures disagreed with the experiment. However, the mobilities for geometries constructed by extending the building pattern found for $n=10-18$ to larger sizes fit the measurements.[60] In LDA, these geometries for $n=19$ and 20 are only a fraction of an eV above the near-spherical global minima. For $n \leqslant 10$, our structures agree with the accepted global minima shown in Fig. 1. [We found C_{2v} (I) for Si_9 and C_{3v} for Si_{10}.]. For $n=11$, we obtained the C_{2v} geometry[5] and an isoenergetic C_s (I) isomer not previously described (see Fig. 2). The C_s (II) isomer (Fig. 1) proposed by Lee *et al.*[19] and Sieck *et al.*[20] lies higher in energy by $\sim$0.25 eV in both LDA and GGA (see Table I). The C_s bicapped tetragonal antiprism also considered for the ground state in Ref. 5 (species 11e in that paper) is higher than our C_s (I) by $\sim$0.4 eV, a value close to $\sim$0.3 eV at the highest level *ab initio* treatment.[5] The DFT energies of our geometries for $12 \leqslant n \leqslant 20$ are significantly lower than those for any structure proposed in the literature. The Si_{14} C_s geometry has also been located by Jackson and co-workers.[20]

However, the mobilities are measured for ions, not for neutrals. The geometries for Si_n^+ with $n \leqslant 7$ have been extensively optimized.[4,62,63] It has been found that, except for $n=6$, the structures remain identical to those of the neutrals. Si_6 rearranges upon charging into a lower-symmetry C_{2v} isomer. Geometries for Si_n with $n \leqslant 10$ and $n=13$ have been relaxed for the cations,[16,17,39,64] but no other structural possibilities have been considered. Here we report the lowest energy geometries found for the cations with $n \leqslant 20$. As described in Sec. II, we have now ventured beyond LDA by employing two different gradient-corrected treatments. In Sec. III, we compare the calculated mobilities for these structures in He gas with the measurements at two different temperatures. The mobility depends on the average collision integral, which in turn depends on the geometry of the ion. The agreement between calculated and measured mobilities is a necessary but not sufficient criterion for the structural assignment, as several low-energy isomers often have very similar mobilities. Hence it is desirable to correlate other properties of the proposed geometries with experiment. In Sec. IV, we compute the ionization potentials of our geometries for $n \leqslant 20$ and compare the values with the measurements. The dissociation pathways and their energies for Si_n clusters will be discussed elsewhere.[65]

II. STRUCTURAL OPTIMIZATION OF THE Si_n CATIONS

A. LDA calculations

The global minima for cluster cations with $n \leqslant 20$ were found by relaxing a number of the low-energy isomers of the neutrals[60] to the nearest local minima (without any symmetry constraints). For $n<12$, we also performed simulated annealing with the Car–Parrinello method where all interatomic interactions were described by LDA. The resulting minima were the same. The total energies were evaluated using the all-electron localized-basis DMOL code.[66] We employed the double numerical plus polarization basis set and the Vosko–Wilk–Nusair (VWN) functional for exchange and correlation. Spin-polarization terms were included. The results for several reasonably low-energy isomers of the neutrals and the cations are listed in Table I.

TABLE I. Cohesive energies (with respect to the spin-polarized isolated neutral atoms) for the low-energy isomers of Si_n ($n \leqslant 20$) neutrals and cations and mobilities for cations.

		Cohesive energy, eV					Inverse mobilities for cations, V^* s/m^2			
		Neutrals		Cations			298 K		78 K	
Size	Point group	LDA[a]	PWB	LDA	PWB	BLYP	Calc.	Exp.	Calc.	Exp.
2		1.968	1.755	−2.003	−2.176	−2.173				
3	C_{2v}	2.929	2.537	0.203	−0.165	−0.236				
4	D_{2h}	3.509	3.042	1.541	1.106	0.968	930	915	705	695
5	D_{3h}	3.791	3.266	2.141	1.642	1.443	1025	1005	760	755
6	D_{4h}	4.001	3.439	2.692	2.145	1.870	1100	1105	810	810
6	C_{2v}	4.001	3.438	2.724	2.187	1.915	1110	1105	815	810
7	D_{5h}	4.147	3.555	2.988	2.410	2.104	1190	1190	865	865
8	C_{2h}	4.090	3.491	3.179	2.596	2.265	1295	1310	925	930
8[b]	C_1/C_s	4.016	3.422	3.185	2.596	2.263	1295	1310	925	930
9	C_{2v} (I)	4.202	3.580	3.354	2.753	2.422	1380	1380	980	975
9	C_{2v} (II)	4.145	3.527	3.332	2.727	2.374	1365	1380	975	975
9	C_s	4.081	3.466	3.284	2.690	2.367	1410	1380	995	975
10	C_{3v}	4.329	3.682	3.527	2.900	2.552	1425	1430	1010	1000
10	T_d	4.260	3.626	3.494	2.874	2.521	1465	1430	1025	1000
11	C_{2v}	4.270	3.618	3.627	2.985	2.619	1520	1515	1065	1055
11	C_s (I)	4.269	3.620	3.667	3.029	2.653	1520	1515	1070	1055
11	C_s (II)	4.247	3.593	3.622	2.973	2.613	1510	1515	1065	1055
12	C_{2v}	4.303	3.648	3.684	3.034	2.667	1605	1615	1125	1115
12	C_s	4.251	3.593	3.694	3.040	2.679	1605	1615	1120	1115
13	C_s	4.303	3.634	3.746	3.093	2.709	1680	1690	1175	1165
13	C_{3v}	4.285	3.624	3.734	3.082	2.707	1685	1690	1170	1165
13	C_{2v}	4.278	3.616	3.751	3.102	2.730	1690	1690	1175	1165
14	C_s	4.348	3.677	3.842	3.181	2.790	1770	1770	1225	1210
15	C_{3v}	4.378	3.701	3.891	3.225	2.829	1845	1855	1275	1260
15	D_{3h}	4.377	3.688	3.878	3.197	2.778	1760	1855	1225	1260
15	C_1	4.367	3.684	3.894	3.219	2.808	1800	1855	1250	1260
16	C_{2h} (I)	4.339	3.659	3.909	3.236	2.843	1935	1945	1330	1315
16	C_{2h} (II)	4.338	3.672	3.925	3.265	2.901	1960	1945	1335	1315
16	C_s	4.336	3.661	3.906	3.240	2.845	1925	1945	1325	1315
16	C_{3v}	4.334	3.642	3.917	3.232	2.809	1845	1945	1280	1315
17	C_{3v}	4.383	3.703	3.970	3.298	2.905	2010	2030	1375	1360
17	C_2	4.364	3.675	3.971	3.291	2.889	1940	2030	1335	1360
18	C_{3v}	4.401	3.720	4.013	3.340	2.941	2190	2120	1510	1425
18	D_{3h}	4.389	3.704	4.006	3.329	2.929	2090	2120	1415	1425
19[c]	C_{2v}	4.412	3.715	4.058	3.369	2.956	2080	2205	1425	1470
19	C_s	4.396	3.709	4.037	3.357	2.956	2190	2205	1485	1470
20	C_s	4.416	3.714	4.081	3.388	2.976	2150	2255	1465	1495
20	C_2	4.399	3.712	4.061	3.381	2.982	2300	2255	1540	1495

[a]The LDA energies in the table differ from those listed in Ref. 60 by a small constant shift due to our use of a different local density functional code.

[b]This isomer has C_s symmetry for cation and C_1 for the neutral.

[c]Same as the near-spherical geometry denoted in Ref. 60 as C_s.

In agreement with the literature,[4,62] we find that the edge-capped trigonal C_{2v} structure, which is nearly degenerate with the D_{4h} isomer for the neutral, becomes a clear global minimum for the Si_6^+. A similar situation, where one of two nearly degenerate isomers for the neutral becomes a definite ground state for the cation, occurs for $n=11$, 15, and 16. For $n=11$, the C_s (I) geometry is now favored by 0.04 eV/atom. For $n=16$, the C_{2h} (II) isomer becomes the global minimum. For $n=8$, 12, and 13, the cation ground states are quite different from the neutrals. The geometry for $n=8$ is a capped pentagonal bipyramid. Interestingly, the C_s structure previously proposed[14,20] for the neutral Si_{12} is actually the global minimum for cation, although it lies over 0.05 eV/atom above the C_{2v} ground state for the neutral. For $n=13$, the C_{2v} geometry that is the third-best for neutral becomes lowest in energy for cation, while the C_{3v} structure of Andreoni and co-workers[13] is the ground state for neither. For $n=15$ and 17, the cations relaxed from a high-energy neutral isomer are almost degenerate with those derived from the neutral global minimum. This cation for $n=17$ belongs to the family of near-spherical clusters that appears in LDA calculations for the neutrals[60] starting from $n=19$. The new lowest energy LDA structures found for cations with $n=8$, 12, 13, 15, and 17 are pictured in Fig. 3.

B. Effect of gradient corrections

Wei *et al.*[64] have evaluated the energies of Si_n clusters up to $n=10$ using the gradient-corrected PLSD (post local

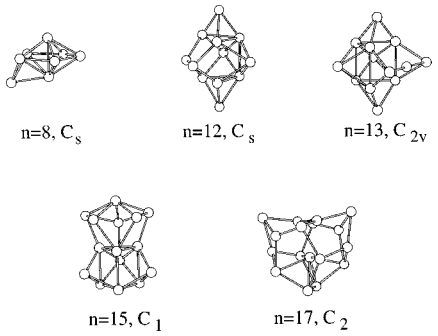

FIG. 3. LDA global minima for Si_n ($n \leqslant 20$) cations that differ from neutrals in Figs. 1 and 2.

spin density) functional. However, these calculations were performed at the LDA geometries, for the lowest energy isomers only. No gradient-corrected DFT treatments have previously been applied to larger silicon clusters. To test the effect of these corrections, we have used two different generalized gradient approximation (GGA) functionals: the Perdew–Wang–Becke 88 (PWB) and Becke–Lee–Yang–Parr (BLYP). Upon full reoptimization of both Si_n and Si_n^+ geometries, we have found that all bond lengths systematically increase, on average, by ~1.5% in PWB and 2.5% in BLYP, as compared with the LDA. While the absolute cohesive energies decrease by some 15%–20% as usual, the relative energetics of different isomers remains remarkably unperturbed in either GGA treatment (Table I). The only noticeable trend is very slight, on the order of one to several hundredths of eV/atom (less than a percent of the total cohesive energy), preference given by both PWB and BLYP to more elongated geometries of either neutrals or cations in the $n \geqslant 15$ size range. This is, however, sufficient to make the C_{3v} and C_{2h} (II) isomers the clear global minima, respectively, for Si_{15} and Si_{16}, and to reverse the change in the ground states of Si_{15} and Si_{17} predicted by LDA to occur upon charging. Also, the C_{2h} and C_s isomers of Si_8^+ become degenerate once the gradient corrections are accounted for.

The introduction of gradient corrections in DFT renders our ''prolate'' geometries for $n=19$ and 20 practically isoenergetic with the ''near-spherical'' species, for either neutrals or cations. We have hypothesized[60] that the ''near-spherical'' isomers are not found experimentally despite being lower in energy according to LDA because they are discriminated against by an entropic effect. The observed isomer distribution is frozen in at or above the energy of the barrier for interconversion. This always favors an isomer with higher vibrational density of states, and lower vibrational frequencies. As would be expected from the general shape considerations, the prolate Si_n isomers have a softer vibrational spectrum than the near-spherical ones.[45] A similar effect substantially delays the onset of structural transition in carbon cluster ions from chains to rings,[67] and from rings and graphite sheets to fullerenes.[68] Besides this phenomenon, the vibrational frequencies also affect the zero-point energies (ZPE) of molecules. In principle, the energies of the different isomers should include ZPEs,[5] while the energies listed in Table I correspond to the bottoms of potential wells. When the average vibrational frequencies of compared geometries are essentially equal, this results in a constant energy shift for all isomers, and the energy ordering is not disturbed. This turns out to be the case when the competing Si_n species are roughly similar in shape.[69] Otherwise, the geometries having lower frequencies have lower ZPEs and are preferred. Our preliminary evaluations based on the vibrational spectra calculated for selected cases indicate that this should additionally favor the prolate isomers in the n ~20 range by several meV/atom.

III. MOBILITIES OF THE SILICON CLUSTER CATIONS

A. Experimental methods

The mobilities of Si_n cations were measured using a tandem quadrupole drift tube apparatus described in detail elsewhere.[70] Briefly, the clusters are generated by pulsed 308 nm laser vaporization of a silicon rod and entrained in a continuous He gas flow. They are mass selected and injected at a controlled energy into a 7.6 cm drift tube containing He buffer gas. The clusters exiting the drift tube are mass selected one more time and detected by an off-axis collision dynode and dual microchannel plates. Mobilities are measured by injecting a 20–50 μs pulse of cluster ions into the drift tube and recording the arrival time distribution at the detector. The drift tube can be cooled using liquid nitrogen. The temperature is monitored by five thermocouples installed along the drift tube. The average of the five values was recorded. The temperature gradient was around 1 K. The drift field, buffer gas pressure, and injection energy were varied in the ranges of 13.3–15.5 V/cm and 2.5–9.4 Torr, and 50–120 eV, respectively, and the measured reduced mobilities remained unchanged. Thus the thermalization length following injection is negligible, the effective length of the drift tube is constant, and the experiments were carried out in the low drift field regime where the mobility is independent of the field.

All the measurements were performed at He buffer gas temperatures of 78 and 298 K. The data at 298 K have already been published,[58,59] while those for 78 K are reported for the first time. The resolving power of mobility measurements is inversely proportional to the square root of buffer gas temperature.[59] Thus cooling of drift tube down to 78 K had improved the resolution by a factor of two, down to ~4%. However, no new isomers were observed.

B. Evaluation of mobilities using trajectory calculations

The structural assignment of features observed in mobility measurements is performed by comparing the measured values with those computed for a number of reasonable candidate geometries. The mobility of a gas phase ion, K, is inversely proportional to the orientationally averaged collision integral,[71] $\Omega_{\mathrm{avg}}^{(1,1)}$,

$$K = \frac{(18\pi)^{1/2}}{16}\left[\frac{1}{m}+\frac{1}{m_B}\right]^{1/2}\frac{ze}{(k_BT)^{1/2}}\frac{1}{\Omega_{\mathrm{avg}}^{(1,1)}}\frac{1}{N}.$$

Here m and m_b are, respectively, the masses of the ion and of the buffer gas atom, ze is the ionic charge, N is the buffer gas number density, and T is the gas temperature.

The collision integral is evaluated by numerically integrating the momentum transfer cross section over the Maxwellian distribution of relative velocities between the buffer gas and the ion. This cross section is calculated by averaging a function of the scattering angle over the impact parameter and collision geometry. The scattering angles are determined by propagating classical trajectories of He atoms in their intramolecular potential with the polyatomic ion.[72] This potential is constructed as a sum of pairwise Lennard-Jones interactions plus a charge-induced dipole term. In our preliminary communication,[60] we assumed uniform delocalization of ionic charge over all cluster atoms. However, it has been shown that localization of the charge on specific atoms may substantially affect the mobility.[73] Hence we presently use the Milliken populations obtained from DFT (the populations produced by LDA and both gradient-corrected functionals are essentially identical). Calculations show almost equal partial charges on all atoms in small clusters, but starting from about $n=9$ the ionic charge becomes increasingly localized on just a few atoms. At room temperature, this causes a slight (within 1%) increase in the collision integrals for the larger species. As for the carbon clusters,[73] the magnitude of this effect increases at lower temperatures, reaching 2.5% for $Si_{18}^+C_{3v}$ at 78 K. The parameters for the Lennard-Jones interactions (the depth ϵ and the intercept at $\epsilon=0$, σ) were fit to reproduce the mobilities of Si_7 cation at both 78 and 298 K. A system of two equations with two variables has to be satisfied, thus our fit of $\epsilon=1.38$ meV and $\sigma=3.47$ Å is unique.[74]

It is really necessary to compare the calculated mobilities with the measurements at two significantly different temperatures. This is because our argument hinges on the assumption that the additive pairwise Lennard-Jones potential that was fit for the small clusters remains valid for larger ones. The interaction potential could conceivably change in a way that would coincidentally produce the right mobility for a wrong structure at a particular temperature. This, however, cannot happen at two different temperatures simultaneously.

C. Structural assignments

The mobilities for our low-energy Si_n^+ geometries for $n \leqslant 20$ are compared with the measurements at 298 and 78 K in Table I. The overall agreement at 298 K is substantially better than that we reported previously[60] using the neutral geometries. The improvement is mostly thanks to the introduction of gradient corrections into cluster geometries, with the effect of charge localization being relatively minor. For all species smaller than Si_{18}^+, the mobilities computed at both 78 and 298 K for the lowest energy (in GGA) geometries are within 2% of the experiment, a generally accepted error margin.[67a,75] In fact, the mean relative deviation from the measurements for $n=4-17$ is only ~0.7%, a value close to the experimental accuracy. The collision integrals calculated for the tetracapped octahedron structure of Si_{10}^+ exceed the measurements at both temperatures by 2.5%, which virtually excludes this isomer. The agreement for the Si_9^+ tricapped octahedron is borderline at either 298 or 78 K. Unfortunately, the difference in mobilities between other reasonably low energy isomers for $n \leqslant 13$ is insufficient to unambiguously confirm our calculated global minima. For $n=15$ and 17, the cation isomers that are lowest energy in LDA and second lowest in GGA (see Fig. 3) are disqualified, as their calculated room temperature mobilities deviate from the experiment by 3%–5%. Similarly, the collision integrals calculated at 298 K for the near-spherical isomers of Si_{19}^+ and Si_{20}^+ that are global minima in LDA are too small by ~5%. This proves the critical importance of gradient corrections in obtaining the right global minima for silicon clusters. Our lowest energy (whether in LDA or GGA) C_{3v} geometry for $n=18$ is outside of the acceptable range of mobilities; however, the second lowest D_{3h} isomer agrees with the experiment better. It is possible that the ground state for Si_{18}^+ has not been located.

To put the results for our geometries into perspective, we have calculated the mobilities for a number of Si_n structures from the literature. We have already shown[60] that cross sections determined for the ''alternating stacked triangles'' of Grossman and Mitas[43] are smaller than the measurements at 298 K by 5%–10%, hence these structures are not elongated enough. In contrast, the values for ''stacked puckered sixfold rings'' of Kaxiras and Jackson[42,45] are too large by 5%–15%, so these geometries are too long.[60] The family of ''stacked triangles'' [43] lies higher in energy than our ''stacked Si_9 TTP units'' by 0.08–0.2 eV/atom (in LDA) in the $n=14-26$ range, and that of ''sixfold rings'' [42,45] for $n=20-26$ is above our geometries by at least 0.1 eV/atom. The especially low reactivities of Si_n^+ with $n=13$, 19, and 23 toward ethylene,[76,77] oxygen,[77–79] ammonia,[80] and water[77,78,81] had prompted a hypothesis of the icosahedral packing for silicon clusters,[32,34b,82] where these sizes would correspond to the closure of geometric (sub)shells. However, the Si_{13} I_h is an extraordinarily high energy geometry in both LDA[13,16,17,39] and *ab initio* calculations,[43,83] and is in fact not even a stationary point. While its energy relative to the ground state decreases for the cation, it still remains about 0.1 eV/atom above the minimum.[16,17] We can now rule out the icosahedral growth pattern experimentally: the cross sections calculated for these structures at 298 K are below the true values by 4% for Si_{13} and by over 10% for Si_{19} and Si_{23}. Any silicon clusters adopting the tetrahedral network of the bulk can also be eliminated. For example, the room temperature collision integrals for the Si_{10} adamantane geometry and the conventionally bound D_{2h} isomer[25] are 11%–12% above the measured values.

The mobilities of polyatomic ions have often been calculated using the projection approximation,[67,75] where the collision integral is equated to the orientationally averaged projection of an ion on a plane. We have already demonstrated that this method is generally inadequate for the evaluation of mobilities for carbon cluster ions, as the errors for some geometries exceed 10%.[72,73,84] If the projection approximation is used for silicon clusters, the collision integrals for all species with $n>7$ are increasingly underestimated, a trend analogous to that observed for the progression

TABLE II. Calculated ionization potentials (eV) for Si_n clusters up to $n=20$.

Size	Point group	Our LDA, AIP–VIP	Our PWB, AIP–VIP	PLSD,[a] AIP-VIP	OVGF, VIP[b]	MP4, VIP[c]	TB,[d] VIP[e]	TB,[f] VIP
1		8.29	8.30	8.53		8.0		
2		7.94–7.94	7.86–7.87	8.04-8.14		7.5	8.09/8.28	8.24
3	C_{2v}	8.18–8.27	8.11–8.20	8.36-8.47	8.14	7.9	8.11/8.38	8.49
4	D_{2h}	7.87–8.17	7.74–8.06	7.99-8.28	8.11	7.6	7.70/8.02	7.95
5	D_{3h}	8.25–8.32	8.12–8.18	8.22-8.42	8.19	7.8	8.07/8.08	8.53
6	D_{4h}	7.85–7.99	7.76–7.89			7.5	8.27/8.52	8.42
6	C_{2v}	7.66–7.98	7.51–7.54	7.70-8.18	7.81			
7	D_{5h}	8.11–8.14	8.02–8.04	8.04-8.24	7.83		7.73/7.77	8.08
8	C_{2h}	7.29–7.44	7.16–7.30	7.39-7.57	7.44		7.12/7.19	7.80
8[g]	C_1/C_s	6.65–7.32	6.61–7.18					
9	C_{2v} (I)	7.63–7.75	7.44–7.57				7.43/7.52	
9	C_{2v} (II)	7.32–7.50	7.20–7.41	7.25-7.60			7.10/7.12	
9	C_s	7.17–7.51	6.98–7.35		7.17			
10	C_{3v}	8.02–8.08	7.82–7.91	7.84-8.21	7.92		7.36/7.53	
10	T_d	7.66–7.68	7.52–7.52				7.27/7.34	
11	C_{2v}	7.07–7.20	6.96–7.06					
11	C_s (I)	6.62–6.82	6.50–6.72					
11	C_s (II)	6.88–7.16	6.82–7.07					
12	C_{2v}	7.43–7.60	7.37–7.45					
12	C_s	6.68–6.89	6.64–6.76					
13	C_s	7.24–7.48	7.03–7.32					
13	C_{3v}	7.16–7.29	7.05–7.20					
13	C_{2v}	6.85–7.03	6.68–6.84					
14	C_s	7.08–7.41	6.94–7.31					
15	C_{3v}	7.31–7.51	7.14–7.40					
15	D_{3h}	7.50–7.52	7.37–7.41					
15	C_1	7.10–7.51	6.98–7.43					
16	C_{2h} (I)	6.88–6.95	6.77–6.90					
16	C_{2h} (II)	6.61–6.66	6.51–6.58					
16	C_s	6.88–7.10	6.74–7.02					
16	C_{3v}	6.67–6.74	6.56–6.64					
17	C_{3v}	7.02–7.19	6.89–7.07					
17	C_2	6.68–6.79	6.53–6.63					
18	C_{3v}	6.98–7.03	6.84–6.91					
18	D_{3h}	6.89–6.94	6.75–6.79					
19[g]	C_{2v}	6.73–6.83	6.57–6.75					
19	C_s	6.82–6.96	6.69–6.81					
20	C_s	6.70–6.86	6.52–6.76					
20	C_2	6.76–6.83	6.62–6.79					

[a]Reference 64.
[b]Reference 87.
[c]Reference 1.
[d]Reference 86.
[e]Two values correspond to two different tight-binding parameterizations.
[f]Reference 85.
[g]See footnotes (b) and (c) to Table I.

of carbon fullerenes.[72] This would erroneously disqualify most of our ''stacked TTP'' structures, while some of the ''puckered sixfold rings'' [42,45] would appear as viable candidates. So silicon clusters are yet another system where the projection approximation would mislead the structural assignments.

IV. IONIZATION POTENTIALS OF SILICON CLUSTERS

A. Calculation of ionization potentials

Mobility measurements can only probe the structures of charged clusters. It is apparent from Sec. II that the geometries of some Si_n cations could be quite different from the respective neutrals. The structural candidates found for the neutral clusters could possibly be distinguished using the ionization potentials (IPs). Furthermore, if the calculated IPs reproduce all the local variations in the measured values, this would constitute indirect evidence that the neutral geometries are correct. The IPs of silicon clusters have previously been modeled using tight binding (TB),[85,86] MP4 perturbation theory,[1] LDA and gradient-corrected PLSD,[64] and the outer valence Green function (OVGF) technique.[87] All these calculations were limited to $n \leqslant 10$, except for TB,[85,86] which also studied $n=11$ and 12. However, the icosahedron-based TB geometries assumed[85,86] for $n>10$ are very high in energy. Here we analyze the IPs of our optimized Si_n clusters[60] for $n \leqslant 20$ and compare them with the measurements.

Ionization potentials of silicon clusters have been measured by threshold photoionization.[54–57] Ideally, if the internal temperature of the neutral is close to absolute zero and

the true threshold is identified, the measurement would provide the adiabatic ionization potential (AIP). If the geometry changes significantly upon ionization, the true threshold would probably not be located, and the measured value would lie between the AIP and the vertical ionization potential (VIP).[88] We have computed both using LDA and PWB (see Table II). The AIPs were evaluated by relaxing the ionized clusters toward the nearest local minimum without any symmetry constraints.[89] Ionization potentials derived using PWB are below the LDA values by 0.05–0.2 eV, but all the size-dependent features are retained. The difference between the AIPs and the VIPs turned out to be small, ranging from under 0.03 eV for Si_2, Si_7, and Si_{10} T_d to 0.2–0.3 eV. For Si_8 C_s, the difference is exceptionally large, 0.6–0.7 eV. So the uncertainty introduced into the comparison between our calculations and experiment by the doubt as to which IP had been measured is usually small. In the range of comparison, the calculated IPs exhibit the same size-dependent trend as the results of previous first-principles calculations,[1,64,87] although the absolute values differ (see Table II).

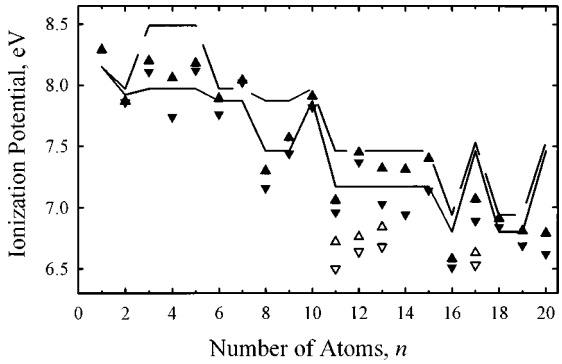

FIG. 4. Ionization potentials of silicon clusters. For $n \geq 3$, solid and dashed lines are the lower and upper boundaries obtained in the bracketing experiments of Fuke *et al.* (Ref. 56). The limits for $n=3$ and 11 were adjusted on the basis of raw data (Ref. 56) (see Ref. 57 and Note 48 in Ref. 62). The value for the dimer is from the more accurate measurements (Ref. 57) and that for the atom is from Ref. 90. Triangles are the vertical (▲) and adiabatic (▼) IPs computed using the gradient-corrected PWB functional for our neutral geometries. Filled symbols are for the lowest energy isomers (in GGA), empty ones are for the $Si_{11}C_s$ (I), $Si_{12}C_s$, $Si_{13}C_{2v}$, and $Si_{17}C_2$. For $n=19$ and 20, the ''prolate'' structures are assumed.

B. Structural assignments

The IPs computed for the lowest energy Si_n clusters ($n \leqslant 20$) using PWB are compared with the measurements in Fig. 4. All size-dependent experimental features for $n \leqslant 19$ are reproduced by our calculations at least qualitatively, including the ''plateau'' for $n \geqslant 12$ pointed out by Fuke *et al.*[56] Unfortunately, the error margin of absolute values on the order of 0.4 eV (based on the data for $n=16$ and 17) and a fairly broad experimental bracketing limit the utility of the presently available data in distinguishing between different geometries. Also, a threshold measurement on an isomeric mixture would reveal the species with the lowest IP, even if its relative abundance is minor. Still, the IPs calculated for Si_{11} C_s (I) and Si_{12} C_s geometries do not agree with the experiment nearly as well as those for the C_{2v} isomers (see Fig. 4). For $n=12$, this result is in accord with our DFT calculations showing the C_{2v} structure to be substantially lower in energy. For $n=11$, C_{2v} and C_s (I) isomers are essentially degenerate for the neutral in both LDA and GGA. The C_s (tricapped octahedron) could also be ruled out for Si_9 on the basis of a more accurate OVGF value for the VIP.[87] The IPs of Si_{17} C_2 are low enough for this geometry to be dismissed (Fig. 4), which seconds the conclusion derived from mobility measurements. The IPs calculated for our lowest energy ''prolate'' and ''near-spherical'' isomers[60] of Si_{19} and Si_{20} are quite close. Both are in a good agreement with the experiment for $n=19$, but the kink observed for $n=20$ is not reproduced by either geometry. The mobilities calculated for our prolate Si_{20} isomer do not match the measurements well, either (Table I). Considering that our ''prolate'' structures for $n=19$ and 20 do not result from any global optimization procedure,[60] it would be hardly surprising if these turn out to be only local (albeit very low) minima. The real threshold (rather than bracketing) IP measurements for silicon clusters that normally have an error margin of ~0.1 eV would likely allow one to extract a lot more structural information from our calculations.

V. SUMMARY

We have searched for the global minima of Si_n cations in the $n \leqslant 20$ size range using DFT-LDA and generalized gradient approximation. The geometries resulting for $n \leqslant 18$ generally resemble the stacked tricapped trigonal prism structures previously found for the neutrals. However, the clusters with 6, 8, 11, 12, and 13 atoms rearrange upon charging. For both neutrals and cations with $n=19$ and 20, the ''prolate'' and ''spherical'' isomers become practically isoenergetic in GGA, whereas LDA clearly prefers the latter. The mobilities in He for the cation structures have been evaluated by the trajectory method, incorporating now the theoretical distribution of ionic charge over the cluster atoms. The mobilities for our lowest energy Si_n^+ geometries with $n<18$ are in excellent agreement with the measurements. The incorporation of gradient corrections in DFT is critically important in finding the global minima for some sizes, for both neutrals and cations. Vertical and adiabatic ionization potentials have been calculated for a number of low-energy Si_n isomers in the $n \leqslant 20$ range. The IPs for our lowest energy neutrals with $n \leqslant 19$ reproduce all size-dependent features observed in the threshold photoionization experiments. Comparison of calculated IPs with the measurements supports the structural assignments for Si_9, Si_{11}, Si_{12}, and Si_{17} in particular.

ACKNOWLEDGMENTS

We are grateful to Professor K. A. Jackson and A. Sieck for providing us with their calculated vibrational frequencies for a number of silicon clusters, and to Professor A. Freeman, Dr. L. Norris, Dr. M. R. Pederson, Dr. V. Rassolov, Professor M. A. Ratner, and Professor G. C. Schatz for useful discussions. This research was supported by the National Science Foundation (Grant No. CHE-9618643), the Army Research Office (DAAG 55-97-1-0133), the Office of Basic Energy Sciences, and the High Performance Computing and

Communications initiative. K.M.H. would like to thank the hospitality of the Hong Kong University of Science and Technology during the preparation of this manuscript.

[1] K. Raghavachari and V. Logovinsky, Phys. Rev. Lett. **55**, 2853 (1985).
[2] K. Raghavachari, J. Chem. Phys. **84**, 5672 (1986).
[3] K. Raghavachari and C. M. Rohlfing, J. Chem. Phys. **89**, 2219 (1988).
[4] K. Raghavachari, Z. Phys. D **12**, 61 (1989).
[5] C. M. Rohlfing and K. Raghavachari, Chem. Phys. Lett. **167**, 559 (1990).
[6] K. Raghavachari and C. M. Rohlfing, Chem. Phys. Lett. **198**, 521 (1992).
[7] K. Raghavachari, Phase Transit. **24–26**, 61 (1990).
[8] G. Pacchioni and J. Koutecky, J. Chem. Phys. **84**, 3301 (1986).
[9] D. Tomanek and M. A. Schluter, Phys. Rev. Lett. **56**, 1055 (1986); Phys. Rev. B **36**, 1208 (1987).
[10] O. F. Sankey, D. J. Niklewski, D. A. Drabold, and J. D. Dow, Phys. Rev. B **41**, 12750 (1990).
[11] R. Fournier, S. B. Sinnott, and A. E. DePristo, J. Chem. Phys. **97**, 4149 (1992).
[12] P. Ballone, W. Andreoni, R. Car, and M. Parrinello, Phys. Rev. Lett. **60**, 271 (1988); W. Andreoni and G. Pastore, Phys. Rev. B **41**, 10 243 (1990).
[13] (a) W. Andreoni, Z. Phys. D **19**, 31 (1991); (b) U. Rothlisberger, W. Andreoni, and P. Giannozzi, J. Chem. Phys. **96**, 1248 (1992).
[14] M. V. Ramakrishna and A. Bahel, J. Chem. Phys. **104**, 9833 (1996).
[15] N. Binggeli, J. L. Martins, and J. R. Chelikowsky, Phys. Rev. Lett. **68**, 2956 (1992); J. R. Chelikowsky and N. Binggeli, Mater. Sci. Forum **232**, 87 (1996).
[16] J. R. Chelikowsky, N. Binggeli, and K. M. Glassford, Z. Phys. D **26**, 51 (1993).
[17] N. Binggeli and J. R. Chelikowsky, Phys. Rev. B **50**, 11764 (1994).
[18] P. Ordejon, D. Lebedenko, and M. Menon, Phys. Rev. B **50**, 5645 (1994).
[19] I. H. Lee, K. J. Chang, and Y. H. Lee, J. Phys.: Condens. Matter **6**, 741 (1994).
[20] A. Sieck, D. Porezag, T. Frauenheim, M. R. Pederson, and K. Jackson, Phys. Rev. A **56**, 4890 (1997).
[21] I. Vasiliev, S. Ögüt, and J. R. Chelikowsky, Phys. Rev. Lett. **78**, 4805 (1997).
[22] A. Bahel, J. Pan, and M. V. Ramakrishna, Mod. Phys. Lett. B **9**, 811 (1995).
[23] T. Slee, L. Zhenyang, and D. M. P. Mingos, Inorg. Chem. **28**, 2256 (1989).
[24] L. Goodwin, A. J. Skinner, and D. G. Pettifor, Europhys. Lett. **9**, 701 (1989); K. Laasonen and R. M. Nieminen, J. Phys.: Condens. Matter **2**, 1509 (1990); S. Erkoc, Z. Phys. D **19**, 423 (1991); C. R. Zacharias, M. R. Lemes, and A. Dal Pino, Jr., J. Mol. Struct.: THEOCHEM **430**, 29 (1998).
[25] C. H. Patterson and R. P. Messmer, Phys. Rev. B **42**, 7530 (1990).
[26] S. Saito, S. Ohnishi, C. Satoko, and S. Sugano, J. Phys. Soc. Jpn. **55**, 1791 (1986); Z. Phys. D **14**, 237 (1989).
[27] J. A. Niesse and H. R. Mayne, Chem. Phys. Lett. **261**, 576 (1996).
[28] T. T. Rantala, D. A. Jelski, and T. F. George, J. Cluster Sci. **1**, 189 (1990).
[29] I. Kwon, R. Biswas, C. Z. Wang, K. M. Ho, and C. M. Soukoulis, Phys. Rev. B **49**, 7242 (1994).
[30] J. R. Chelikowsky and R. Redwing, Solid State Commun. **64**, 843 (1987); J. R. Chelikowsky, Phys. Rev. Lett. **60**, 2669 (1988).
[31] J. R. Chelikowsky, J. C. Phillips, M. Kamal, and M. Strauss, Phys. Rev. Lett. **62**, 292 (1989).
[32] J. R. Chelikowsky and J. C. Phillips, Phys. Rev. Lett. **63**, 1653 (1989); Phys. Rev. B **41**, 5735 (1990).
[33] J. R. Chelikowsky, K. M. Glassford, and J. C. Phillips, Phys. Rev. B **44**, 1538 (1991).
[34] (a) J. C. Phillips, J. Chem. Phys. **87**, 1712 (1987); (b) Phys. Rev. B **47**, 14132 (1993).
[35] A. Bahel and M. V. Ramakrishna, Phys. Rev. B **51**, 13849 (1995).
[36] A. D. Mistriotis, N. Flytzanis, and S. C. Farantos, Phys. Rev. B **39**, 1212 (1989).
[37] S. Li, R. L. Johnston, and J. N. Murrell, J. Chem. Soc., Faraday Trans. **88**, 1229 (1992); D. J. Wales and M. C. Waterworth, *ibid.* **88**, 3409 (1992).
[38] K. Jug, J. Mol. Struct.: THEOCHEM **202**, 277 (1989); H. Kupka and K. Jug, Z. Phys. D **13**, 301 (1989); Chem. Phys. **130**, 23 (1989); H. J. Nolte and K. Jug, J. Chem. Phys. **93**, 2584 (1990); K. Jug and U. Wolf, Chem. Phys. **163**, 69 (1992).
[39] B. L. Gu, Z. Q. Li, and J. L. Zhu, J. Phys.: Condens. Matter **5**, 5255 (1993).
[40] X. G. Gong, Q. Q. Zheng, and Y. Z. He, J. Phys.: Condens. Matter **7**, 577 (1995).
[41] D. A. Jelski, Z. C. Wu, and T. F. George, Chem. Phys. Lett. **150**, 447 (1988).
[42] E. Kaxiras and K. A. Jackson, Z. Phys. D **26**, 346 (1993); Phys. Rev. Lett. **71**, 727 (1993).
[43] J. C. Grossman and L. Mitas, Phys. Rev. Lett. **74**, 1323 (1995); Phys. Rev. B **52**, 16735 (1995).
[44] M. Menon and K. R. Subbaswamy, Phys. Rev. B **50**, 11577 (1994); **55**, 9231 (1997).
[45] M. R. Pederson, K. Jackson, D. V. Porezag, Z. Hajnal, and T. Frauenheim, Phys. Rev. B **54**, 2863 (1996).
[46] J. Song, S. E. Ulloa, and D. A. Drabold, Phys. Rev. B **53**, 8042 (1996).
[47] E. C. Honea, A. Ogura, C. A. Murray, K. Raghavachari, W. O. Sprenger, M. F. Jarrold, and W. L. Brown, Nature (London) **366**, 42 (1993).
[48] S. Li, R. J. Van Zee, W. Weltner, Jr., and K. Raghavachari, Chem. Phys. Lett. **243**, 275 (1995).
[49] (a) C. C. Arnold and D. M. Neumark, J. Chem. Phys. **99**, 3353 (1993); (b) C. Xu, T. R. Taylor, G. R. Burton, and D. M. Neumark, *ibid.* **108**, 1395 (1998); (c) O. Chesnovsky, S. H. Yang, C. L. Pettiette, M. J. Craycraft, Y. Liu, and R. E. Smalley, Chem. Phys. Lett. **138**, 119 (1987).
[50] R. Kishi, H. Kawamata, Y. Negishi, S. Iwata, A. Nakajima, and K. Kaya, J. Chem. Phys. **107**, 10029 (1997).
[51] L. A. Bloomfield, R. R. Freeman, and W. L. Brown, Phys. Rev. Lett. **54**, 2246 (1985); W. Begemann, K. H. Meiwes-Broer, and H. O. Lutz, *ibid.* **56**, 2248 (1986).
[52] Q. L. Zhang, Y. Liu, R. F. Curl, F. K. Tittel, and R. E. Smalley, J. Chem. Phys. **88**, 1670 (1988).
[53] M. F. Jarrold and E. Bower, J. Phys. Chem. **92**, 5702 (1988); M. F. Jarrold and E. C. Honea, *ibid.* **95**, 9181 (1991).
[54] J. R. Heath, Y. Liu, S. C. O'Brien, Q. L. Zhang, R. F. Curl, F. K. Tittel, and R. E. Smalley, J. Chem. Phys. **83**, 5520 (1985).
[55] D. J. Trevor, D. M. Cox, K. C. Reichmann, R. O. Brickman, and A. Kaldor, J. Phys. Chem. **91**, 2598 (1987).
[56] K. Fuke, K. Tsukamoto, and F. Misaizu, Z. Phys. D **26**, S204 (1993); K. Fuke, K. Tsukamoto, F. Misaizu, and M. Sanekata, J. Chem. Phys. **99**, 7807 (1993).
[57] C. B. Winstead, S. J. Paukstis, and J. L. Gole, Chem. Phys. Lett. **237**, 81 (1995); A. Marijnissen and J. J. ter Meulen, *ibid.* **263**, 803 (1996).
[58] M. F. Jarrold and V. A. Constant, Phys. Rev. Lett. **67**, 2994 (1991).
[59] M. F. Jarrold and J. E. Bower, J. Chem. Phys. **96**, 9180 (1992).
[60] K. M. Ho, A. A. Shvartsburg, B. Pan, Z. Y. Lu, C. Z. Wang, J. G. Wacker, J. L. Fye, and M. F. Jarrold, Nature (London) **392**, 582 (1998).
[61] M. F. Jarrold, in Cluster Ions, edited by C. Y. Ng, T. Baer, and I. Powis (Wiley, Chichester, 1993), p. 166.
[62] R. Kishi, Y. Negishi, H. Kawamata, S. Iwata, A. Nakajima, and K. Kaya, J. Chem. Phys. **108**, 8039 (1998).
[63] M. Woeller, M. Muhlhauser, S. D. Peyerimhoff, and F. Grein, Chem. Phys. Lett. **288**, 603 (1998).
[64] S. Wei, R. N. Barnett, and U. Landman, Phys. Rev. B **55**, 7935 (1997).
[65] A. A. Shvartsburg, M. F. Jarrold, B. Liu, Z.-Y. Lu, C.-Z. Wang, and K.-M. Ho, Phys. Rev. Lett. (submitted).
[66] DMOL package, V96.0/4.0.0 (Molecular Simulations Inc., San Diego, CA, 1995).
[67] G. von Helden, M. T. Hsu, N. Gotts, and M. T. Bowers, J. Phys. Chem. **97**, 8182 (1993); G. von Helden, N. G. Gotts, W. E. Palke, and M. T. Bowers, Int. J. Mass Spectrom. Ion Processes **138**, 33 (1994).
[68] J. M. L. Martin, J. El-Yazal, and J. P. Francois, Chem. Phys. Lett. **248**, 345 (1996); **252**, 9 (1996).
[69] K. A. Jackson, M. R. Pederson, D. Porezag, Z. Hajnal, and T. Frauenheim, Phys. Rev. B **55**, 2549 (1997).
[70] M. F. Jarrold, J. Phys. Chem. **99**, 11 (1995).
[71] E. A. Mason and E. W. McDaniel, *Transport Properties of Ions in Gases* (Wiley, New York, 1988).
[72] M. F. Mesleh, J. M. Hunter, A. A. Shvartsburg, G. C. Schatz, and M. F. Jarrold, J. Phys. Chem. **100**, 16082 (1996).
[73] A. A. Shvartsburg, G. C. Schatz, and M. F. Jarrold, J. Chem. Phys. **108**, 2416 (1998).
[74] These values marginally differ from $\epsilon = 1.35$ meV and $\sigma = 3.50$ Å used in our earlier work (Ref. 60), primarily due to the longer bonds in Si_7 optimized using gradient-corrected techniques. Here and for the rest of the paper, the mobilities of our optimized clusters were calculated for the averages of PWB and BLYP geometries. For consistency, the LDA structures from the literature have also been scaled appropriately.

[75] G. von Helden, T. Wyttenbach, and M. T. Bowers, Science **267**, 1483 (1995).
[76] M. F. Jarrold, J. E. Bower, and K. M. Creegan, J. Chem. Phys. **90**, 3615 (1989); K. M. Creegan and M. F. Jarrold, J. Am. Chem. Soc. **112**, 3768 (1990).
[77] U. Ray, M. F. Jarrold, K. M. Creegan, and J. E. Bower, Int. J. Mass Spectrom. Ion Processes **100**, 625 (1990).
[78] M. F. Jarrold, U. Ray, and Y. Ijiri, Z. Phys. D **19**, 337 (1991).
[79] M. F. Jarrold, U. Ray, and K. M. Creegan, J. Chem. Phys. **93**, 224 (1990).
[80] U. Ray and M. F. Jarrold, J. Chem. Phys. **93**, 5709 (1990).
[81] U. Ray and M. F. Jarrold, J. Chem. Phys. **94**, 2631 (1990).
[82] T. Lange and T. P. Martin, Angew. Chem. Int. Ed. Engl. **31**, 172 (1992).
[83] K. Raghavachari and C. M. Rohlfing, private communication.
[84] A. A. Shvartsburg, R. R. Hudgins, Ph. Dugourd, and M. F. Jarrold, J. Phys. Chem. A **101**, 1684 (1997).
[85] J. Zhao, X. Chen, Q. Sun, F. Liu, and G. Wang, Phys. Lett. A **198**, 243 (1995).
[86] C. Jo and K. Lee, J. Korean Phys. Soc. **32**, 182 (1998).
[87] W. von Niessen and V. G. Zakrzewski, J. Chem. Phys. **98**, 1271 (1993).
[88] In principle, the IP measurement for ions at a finite temperature is always an underestimation. However, the clusters had been cooled to ~80 K (Ref. 56) thus the threshold would be lowered by a couple hundredths of an eV at most.
[89] Of course, these AIPs are not always truly adiabatic, as that local minimum is not necessarily the global minimum for cation. However, the wave function of a neutral (particularly at low temperatures) would not measurably overlap with that of a cation assuming an entirely different structure, rather than just a minor distortion of the neutral geometry.
[90] C. E. Moore, Natl. Stand. Ref. Data Ser. (U.S., Natl. Bur. Stand.) **34**, 2 (1970).